Distributed Sensor Fusion of Ground and Air Nodes using Vision and Radar Modalities for Tracking Multirotor Small Uncrewed Air Systems and Birds

Chester V. Dolph[1]
NASA Langley Research Center, Hampton, Virginia 23681

Thomas Lombaerts[2], Corey Ippolito[3], Vahram Stepanyan[4], Evan Kawamura[5], Keerthana Kannan[6],
NASA Ames Research Center, Moffett Field, CA, 94035

Bryan Petty[7], George Szatkowski[8], Todd Ferrante[9], Chris Morris[10],
NASA Langley Research Center, Hampton, Virginia 23681

Federica Vitiello [11], Flavia Causa [12], Roberto Opromolla [13], Giancarmine Fasano [14],
University of Naples Federico II, Naples, Italy

High-density airspace operations with multiple aircraft type and potentially noncooperative aircraft require distributed sensor detection and tracking systems to monitor airspace for safe, autonomous flight operations for advanced air mobility, urban air mobility, and high density small uncrewed air systems (SUAS) flight concepts. This work collected data using a distributed radar and camera sensor framework during the NASA Advanced Air Mobility High Density Vertiplex project SUAS flight operation. Node locations include on an onboard SUAS, affixed to the Landing and Impact Research Facility with approximate 200ft elevation, on a tripod on first-floor roof with an approximate elevation of 20 ft, and on a tripod on a concrete pad that is approximately 4 ft above sea level. Each node includes camera, radar, and GPS.

I. Introduction

Advancing autonomous aircraft operations for Urban Aircraft Mobility (UAM) and Small Uncrewed Aircraft Systems (SUAS) is of significant interest to commercial, government, and consumer applications. The NASA Advanced Air Mobility (AAM) project advances concepts needed to autonomously move people and cargo using vertical takeoff and landing aircraft [1] and utilizes SUAS as a surrogate platform as AAM aircraft are in the initial design phases [2]. Sample SUAS applications include package delivery [3] and remote sensing of crops [4], infrastructure [5], and coordinating disaster response for catastrophic events [6]. Autonomous AAM and SUAS will need to navigate in an airspace that will have both cooperative aircraft, i.e. aircraft that transmit their position

[1] Aerospace Engineer, Aeronautics Systems Engineering Branch,AIAA Member.
[2] Aerospace Research Engineer, KBR Wyle Services, Intelligent Systems Division, AIAA Associate Fellow.
[3] Aerospace Scientist, Intelligent Systems Division, AIAA Senior Member.
[4] ESOF40-Technical Advisor, KBR Wyle Services, Intelligent Systems Division.
[5] Computer Engineer, Intelligent Systems Division, NASA Ames Research Center.
[6] Embedded Software Developer, KBR Wyle Services, Intelligent Systems Division.
[7] Aerospace Engineer, Aeronautics Systems Engineering Branch.
[8] Research Engineer, Safety Critical Avionics Branch.
[9] Robotics Engineer, AMA, Aeronautics Systems Engineering Branch.
[10] Embedded Systems Engineer, Safety Critical Avionics Branch.
[11] Graduate Student, University of Naples "Federico II".
[12] Postdoctoral Scholar, University of Naples "Federico II".
[13] Assistant Professor, University of Naples "Federico II".
[14] Associate Professor, University of Naples "Federico II".

and flight plans over a communication network, and non-cooperative aircraft that need to be avoided using onboard sensing systems [7]. Ground-based systems are needed to monitor autonomous takeoff and landing zones, also known as vertiports, to ensure safe operations for shared airspaces of SUAS and AAM aircraft. Fig. 1 shows the integration of AAM and SUAS in a dense urban airspace including multiple vertiports on skyscraper rooftops. At present, both the technology and the regulations needed for dense flight space shown in the AAM graphic are not available. Real-time detect, track, and perceive aircraft and aerial hazards is needed to ensure safety of passengers and people below the flight space. Development of avoidance systems needs to consider the sensors, sensing environment, algorithms, and risk posed by the aircraft to people. Algorithm development and validation requires data from real-world flight tests.

NASA developed the 1 to 6 UAM Maturity Level (UML) scale to map UAM to mature flight operations [8] where 1 is an initial stage with prototyping for future flight operations and 6 is ubiquitous UAM flight operations in the airspace. To advance sensing algorithms in the UML scale, the NASA Distributed Sensing team, partnered with the NASA AAM High Density Vertiplex (HDV) project, collected a dataset to develop real-time detect, track, and classify strategies for AAM and SUAS. The HDV project developed the AAM concept of operations through operating 3-5 SUAS performing complex maneuvers in a dense airspace, including takeoff and landing [9]. This work was completed in support of NASA Transformational Tools and Technologies (TTT) subproject Revolutionary Aviation Mobility (RAM), where one objective is to enable Urban Air Mobility (UAM) through developing the technology of enabling m operators to control N UAM vehicles [10]. In this work, a dataset is collected during HDV experiments using distributed sensors for the future evaluation of a sensing detection tracking pipeline previously developed in simulation [11] [12]. Researchers from the University of Naples "Federico II" participated in the flight campaign and contributed to the subsequent data analysis in [13] [14]. This paper is organized as follows: contributions, related works, techniques, tracker evaluation, and experimental methodology.

Fig. 1: Advanced Air Mobility Mission will enable safe autonomous transportation for people and cargo in a low-altitude dense airspace as shown in this graphic from [15].

II. Contributions and Future Work

Despite decades of research, widespread autonomous SUAS operations do not exist. This work aims to advance autonomous SUAS and AAM through the development of detection, tracking and classification methodologies using distributed ground and air-based nodes that can be used to provide independent vehicle conformance monitoring, augment onboard navigation, as well as tracking non-cooperative aircraft. Outputs from this system could be used in support of Vertiport Automation Systems that are envisioned for high density operations. Key contributions include:

- Development of distributed sensing framework for monitoring vertiports, air traffic corridors, and onboard SAA.
- Execution of field-test to collect data for framework.
- Planning of analysis of distributed sensing dataset.

Future

- Field-testing a distributed sensing framework developed in simulation using data collected during AAM HDV operations using three ground nodes and one air node.
- Performance analysis of different sensing modalities to determine strengths and weaknesses.
- Performance analysis of detection and tracking strategies.
- Analysis of machine learning strategies for classification of aerial objects in the distributed AAM context.
- Mitigating potential radar interference problems.

III. Technical Approach

A. Overview of Distributed Sensing Framework

A distributed sensing framework for AAM needs to address several technical challenges including sensing a variety of aircraft in a dense airspace, serve as an alternate to onboard navigation systems, as GPS in its current implementation is not reliable in an urban environment, and nominal aviation sensors such as radar encounter performance degradation in cluttered environments [2]. The TTT Distributed Sensing (DS) team proposes the structurally adaptive architecture shown in Fig. 2 with these key components: both cooperative and non-cooperative sensing is utilized to ensure safe operations, distributed sensing provides precision navigation to AAM aircraft, landmarks and vertiports serve as navigation aids, and distributed sensing network informs air traffic controllers.

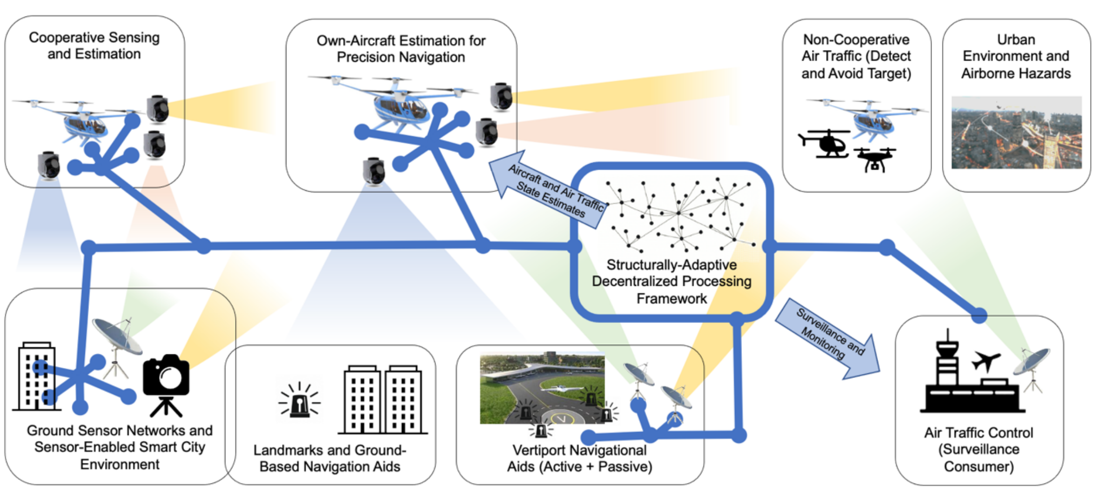

Fig. 2: Distributed Sensing Framework [2].

Key elements of the structurally adaptive decentralized processing framework include the ability for aircraft and operators to exploit distributed sensors in real-time is described in detail in [12]. The flexibility of this framework enables high fidelity position estimation of aircraft as they traverse across an airspace, traversing across varying sensor FOV including ground-based and aerial aircraft. A large set of strategically placed ground sensors and moving air sensors enables higher accuracy for position estimation of aircraft. Further, sensing an aircraft from multiple sensors enhances robustness and safety of the architecture in the event of a single sensor malfunction. Cooperative sensing strategies in [16] [17] develop ground-based sensing techniques to provide an independent method of position estimation for aircraft. Ground-based position estimation can be a backup to onboard navigation systems in the event of a malfunction of GPS. Non-cooperative sensing strategies are needed in the event of an air traffic control outage and provide avoidance of non-cooperative SUAS that do not participate in a traffic management system. The work in [13] compared non-cooperative detect and track strategies of SUAS in the AAM context using visual and radar modalities while the work in [18] developed a sensor fusion method for radar and vision tracking SUAS. Both cooperative and non-cooperative sensing strategies are combined in this framework for precision landing [19] [20].

B. Deployable Distributed Sensing Architecture

Towards advancing UML rating, a distributed sensing architecture was developed based off of the co-located radar and camera prior work in [18]. Objectives of this distributed framework include development of sensing strategies for UAM and SUAS. Four distributed sensor nodes were developed as shown in Fig. 3 during initial checkouts. Each node has a radar, at least 1 global shutter camera, rolling shutter action camera, data recording embedded computer (selected for real-time data-processing capability in the future), and cellular router for remote control of sensor acquisition via SSH using static IP addresses. Sensors and field of view settings are selected to provide sufficient coverage of an airspace surrounding a vertiport for SUAS or UAM aircraft. The sensor details as shown in Table 1 with companion computers and GPS described detailed in Table 2. Three nodes have Sony IMX253 sensors. One node utilizes a Sony IMX304. All nodes utilize an Echodyne Echoflight radar. The payload node uses two Lithium Polymer batteries to supply power for an onboard SUAS configuration or cordless version for field deployment.

Fig. 3: Distributed nodes co-located during initial checkouts.

Table 1: Node Sensor Configuration and typical FOV setting.

Node Description	Camera Model	Camera Resolution (pixels)	Horizontal and vertical Lens FOV (degrees)	Radar model	RADAR FOV (degree)
3 Camera	123S6C-C	4096 × 3000 Each camera	47.3 × 36.1 Each lens	Echoflight	120 × 80
Ground	123S6C-C	4096 × 3000	62.5 × 47.8	Echoflight	120 × 50
Rooftop	122S6C-C	4096 × 3000	62.5 × 47.8	Echoflight	120 × 50
Onboard Payload	123S6C-C	4096 × 3000	62.5 × 47.8	Echoflight	120 × 60

Table 2: Node GPS and Computer Configuration.

Node	GPS Receiver	Data Logging Computer	Cellular Modem
3 Camera	GPS-RTK-SMA ZED-F9P (Ublox)	3 Xaviers with Contech Rogue breakout Board	RUTX11
Ground	GPS-RTK-SMA ZED-F9P (Ublox)	Xaviers with Contech Rogue breakout Board	RUTX11
Rooftop	GPS-RTK-SMA ZED-F9P (Ublox)	NUC 11 Performance Mini Desktop Computer,	RUTX11
Onboard Payload	GPS-RTK-SMA ZED-F9P (Ublox)	Xaviers with Contech Rogue breakout Board	RUTX11

C. HDV Project Objectives

The High Density Vertiplex (HDV) sub-project operated under the Airspace Operations and Safety Program. HDV was tasked with the development, integration assessment of autonomous architecture for UAM operations [21]. HDV broke down the work into different schedule work packages. During the DS data collection, HDV was executing the Scalable Autonomous Operations (SAO) work package with the goal of developing and evaluating a prototype UAM ecosystem for high volume operations at a vertiport, as defined in the HDV CONOPS [22]. A vertiport is the takeoff and landing location for UAS executing UAM operations. This work package consisted of two flight campaigns, the Prototype Assessment Operation (PAO) and the Beyond Visual Line of Sight (BVLOS) operations, which both included simulation and flight activities. The DS team coordinated their data collection with flight operations of HDV during both the PAO and BVLOS flights.

The PAO flight campaign had three main objectives that focused on defining and developing the roles required for high density UAM operations at a vertiport. The first objective was to connect fleet management tools and airspace services to the ground control stations used to execute flight operations. This allowed for fleet managers to issue corrective actions when airspace conflicts occur, allowing the ground control station operators to resolve them. The next objective was to develop a vertiport automation system, which helps the vertiport manager schedule the vertiport operations for vehicles on approach. The final objective for PAO was to demonstrate automation technologies that support high density operations at the vertiport. The HDV team evaluates high density operations by collecting human factors data on the UAM ecosystem.

Following the completion of the PAO flight campaign, the HDV BVLOS flight campaign began. This included establishment of surveillance systems to cover the flight range, development of remote pilot in command training, and flight operations with all flight personnel in a remote operations facility. The surveillance systems on the range included radars and Automatic Dependent Surveillance–Broadcast (ADS-B) sensors for detection of crewed aircraft and Flight Alarm (FLARM) sensors detection of the small UAS. The different sensors were combined and fused on an integrated airspace display for airspace awareness. Remote pilots were trained in the use of the ground control station software and the integrated airspace display to handle nominal and off-nominal flight events during a simulation. The remote pilots then conducted BVLOS flight operations from a remote facility, Remote Operations for Autonomous Missions (ROAM) [23], without any visual observers in the operational area. The range safety officer, responsible for clearing the airspace, was able to use the established surveillance systems to clear the airspace from ROAM.

IV. Experimental Methodology

During flight operations of PAO and BVLOS, the HDV team coordinated scenarios with the DS team. This allowed for the DS team to set up their detection systems, both ground and aerial based, to track the HDV vehicles while they were on their flight path. HDV then provided the GPS positional data from HDV SUAS to the DS for evaluation of the vehicle tracking. Fig. 4 highlights portions of the joint experiment including: the safety pilots bringing 5 SUAS to the vertiport (a), one of the ROAM control rooms (b), an image from the payload on SUAS of the vertiport (c), and HDV+ DS team photo (d). Fig. 5 provides a bird's eye view of the flight range where the red and green lines show the HDV waypoint mission and the yellow pins show the position of the sensors. Sensor placement considerations included capturing the HDV flight ops from multiple poses, aiming to reduce radar interference, elevated positions to reduce ground clutter, safety requirements for SUAS carrying payload, and availability of 120VAC power for ground nodes.

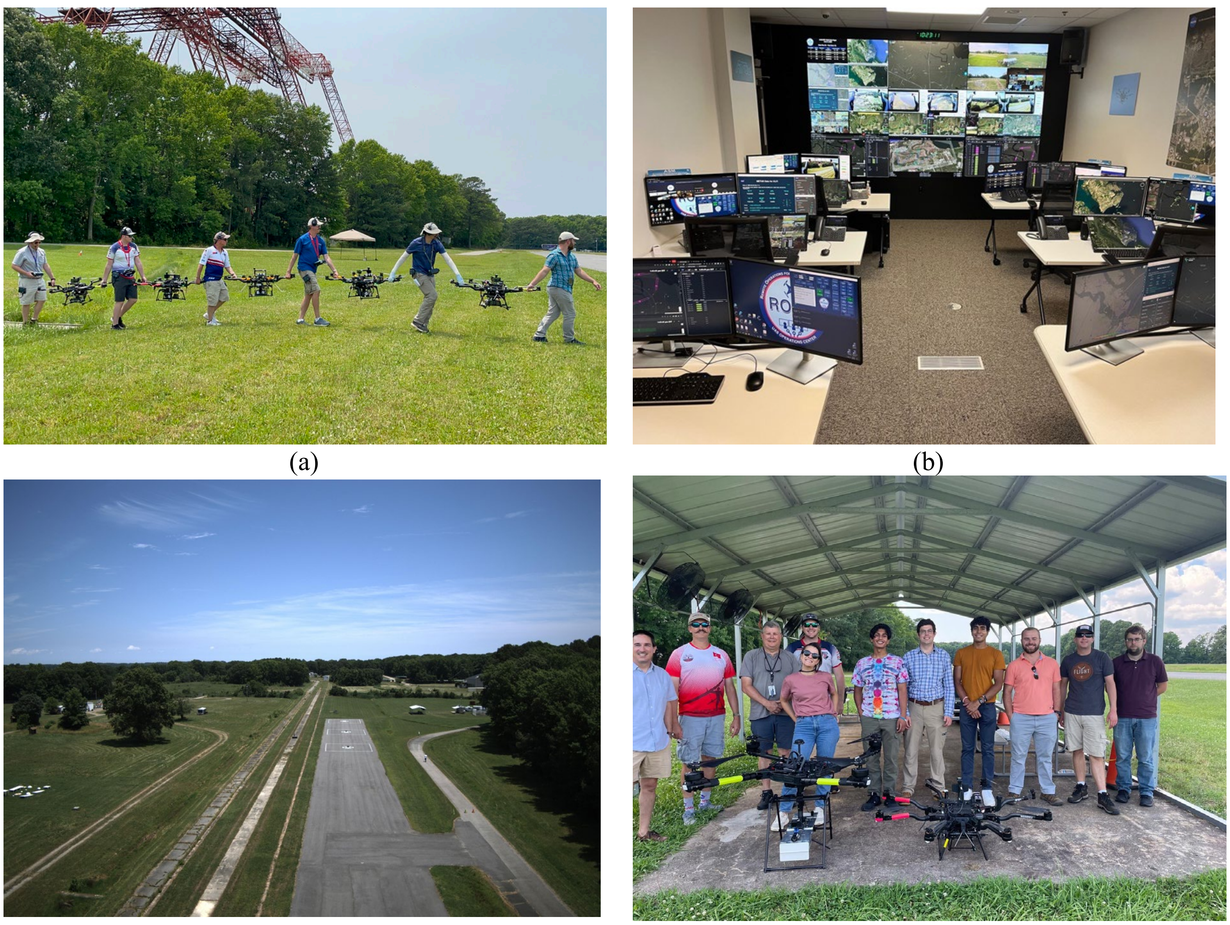

(a) (b)

(c) (d)

Fig. 4: HDV+DS Joint Flight Operations: a) pilot carrying HDV SUAS to vertiport during 5 aircraft operations b) inside of ROAM c) aerial shot of vertiport from Alta X global shutter camera d) HDV + TTT joint flight operations team with Alta X shown with research payload.

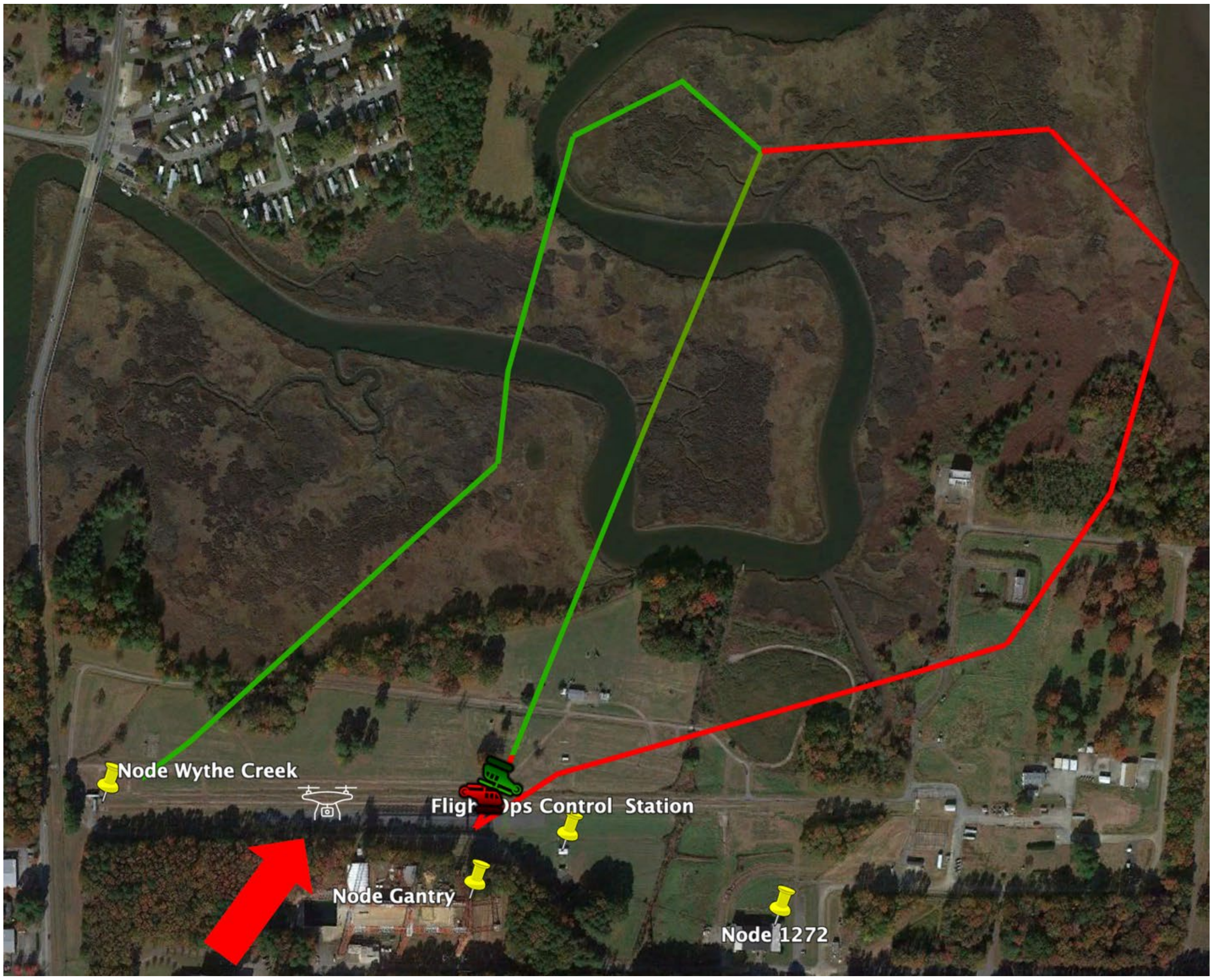

Fig. 5: Overview of SUAS flight operations. SUAS takeoff from the location shown by the two helicopter icons and proceed down the red trajectory path where they will fork to return to the takeoff location or land close to the Wythe Creek location. The arrow shows the location of the SUAS with the onboard payload for the camera and radar.

The ground node configurations are shown in Fig. 6 in their typical position for these experiments. The ground node 3 camera node shown in Fig. 6a includes 3 cameras and 1 radar mounted to Landing and Impact Research Facility (LIRF) structure (also known as the Gantry) with a height of approximately 60m. The three cameras have a 1 degree overlap in field of view yielding a combined horizontal field of view 139.9 with a vertical field of view of 36.1. The ground node is shown in Fig. 6c and is mounted on a deployable tripod. Similarly, the rooftop node is shown in Fig. 6b. Both ground and rooftop nodes use restricted vertical field of view for the radar to avoid returns from ground clutter. Fig. 7 shows the integration of the payload onto the SUAS including the position of radar, camera, embedded computer, and cellular router. Sensors and hardware are held together using aluminum plates. A scope is used to sight the sensor orientation on the ground nodes using landmarks in distance (tree, antenna tower). An inclinometer is used to set elevation angles of the sensor by pitching the tripod head to the nearest $1/10^{th}$ of a degree.

(a)

(b)

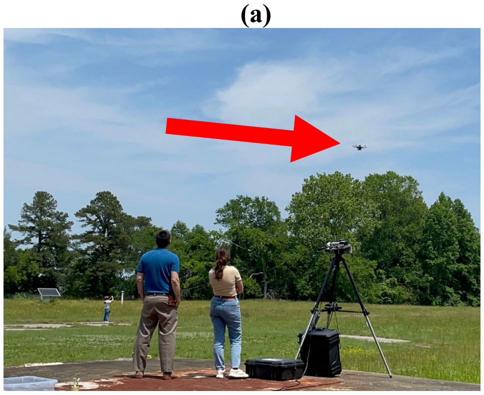

(c)

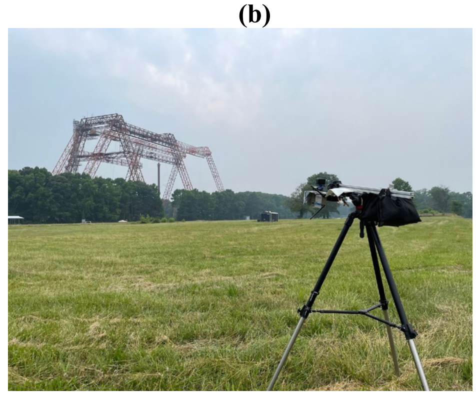

(d)

Fig. 6: Distributed Sensor Nodes: a) Gantry b) rooftop c) ground d) field location for payload powered by LiPo battery.

Integration of the payload is shown in Fig. 7. An isolation mount is used to reduce vibration of the sensor. The radar is cantilevered out from the SUAS vertical center axis to maximize vertical FOV because the SUAS motors have the potential of generating undesired radar detections. The payload is electrically isolated from SUAS avionics. A series of checkout flights in a cage confirmed that radar interference does not pose a problem with the SUAS flight controller and operation of SUAS.

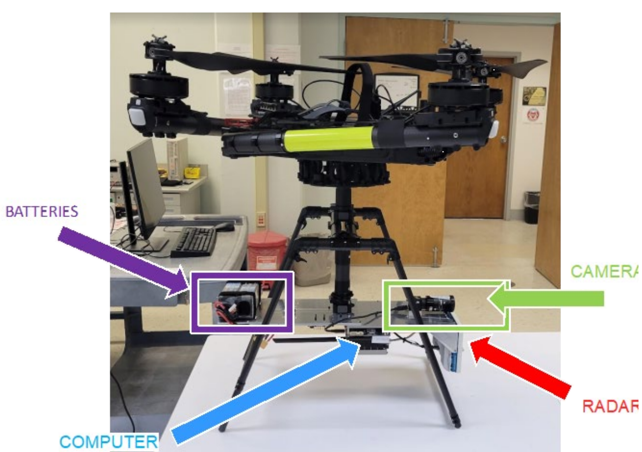

(a)

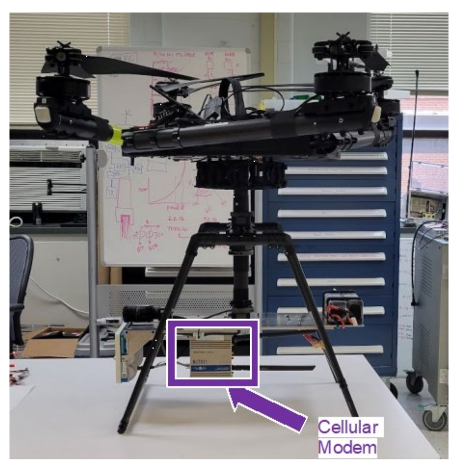

(b)

Fig. 7: Onboard Payload as seen from starboard (a) and port (b) sides with research payload annotated.

The technical specifications of the HDV SUAS are detailed in **Table 3**. The HDV aircraft are shown prior to takeoff at a vertiport in Fig. 8. The technical specifications of the SUAS carrying the payload are shown in **Table 4**, and the aircraft is shown in Fig. 9.

Table 3:Alta 8 specifications.

SUAS Type	Multi-Rotor, 8 Motor(Brushless)
Diagonal Length	52 in (1.3 m)*Does not include Props
Maximum Weight	40 lbs (18.14 kg)
Empty Weight	13.6 lbs (6.2 kg)
Propulsion Battery	6-cell Li-Poly (Nominal 22.2V)
Speed	0 –30 kts (0-15.4m/s)
Max Flight Time	34 mins
Operating Frequency	2.4 GHz RCTX C2 (~2 Miles) 900 MHz C2 & Flight Data (~3 Miles) 700MHz/1700MHz C2 & Flight Data
Command and Control	RC TX Laptop

Fig. 8: Alta 8 on the Vertiports.

Table 4: Alta X specifications.

SUAS Type	Multi-Rotor, 4 Motor (Brushless)
Diagonal Length	89.5 in (2.27 m)
Maximum Weight	76.9 lbs (34.9 kg)
Empty Weight	22.9 lbs (10.4 kg)
Propulsion Battery	12-cell Li-Ion (Nominal 44.4V)
Speed	0 – 38.8 kts (0-20.0m/s)
Max Flight Time	50 mins
Operating Frequency	2.4 GHz RC TX C2 (~2 Miles) FRX 900 MHz Telemetry radio (~1 Mile)
Command and Control	RC TX & Laptop

Fig. 9: Alta X prior to takeoff.

V. Dataset

Approximately 25 terabytes of vision, radar, and GPS data were collected over a period of over 2 months with 9 data collection days as shown in Table 5. Weather conditions varied over the course of this data acquisition. HDV SAO and PAO emphasized certain waypoint patterns that allow for validation of detection and tracking methodologies across weather conditions to confirm algorithm robustness to SUAS sensing in varying backgrounds such as cloudy or partially cloudy. On 5/25/23 and 6/6/2023 2 radars were operated in the same location with varying modes and radar configurations to optimize radar settings. The distributed sensing team operated the Alta X in two flight modes: 1) station keeping to observe PAO/SAO flight operations on 6/13/2023 and 2) head-on collision geometries between Alta X and 1 HDV SUAS with altitude separation of ± 30 ft on 7/11/2023 and 7/26/2023. The payload as configured on the tripod boom in Fig. 6d was tested on 6/6/2023 and 6/9/2023 to test additional distributed sensing scenarios and evaluate radar interference.

Table 5: Dataset Summary. For the Node Location columns, “Y” indicates the radar was transmitting, “N” indicates the radar was off, “2” indicates that two nodes were collocated, and “G” indicates that the SUAS payload was located on the tripod boom. For the Note column, DASC was used in analysis [13] presented at Digital Avionics Systems Conference (DASC), DS-HDV data acquisitions with ground nodes only, and DS-TTT-SAA utilizes the Alta X hovering or completing head-on collision geometries with HDV SUAS.

			Node Location					
Acquisition Number	Date	Time	Wythe	Roof	Gantry	Payload	# HDV SUAS	Note
1	5/17/23	15:16	Y	Y	Y	N	3	Preliminary Checkout
2	5/23/23	15:05	N	2	N	N	2	DASC
3	5/23/23	16:30	N	2	N	N	2	DASC
4	5/25/23	13:23	2	N	N	N	2	DASC
5	5/25/23	14:45	2	N	N	N	2	DASC
6	5/25/23	16:02	2	N	N	N	2	DASC
7	6/6/23	14:00	2	1	1	G	4	DASC
8	6/6/23	15:46	2	1	1	G	4	DASC
9	6/8/23	12:10	1	1	N	N	5	DS-HDV
10	6/9/23	11:00	1	1	1	G	5	DS-HDV
11	6/9/23	13:37	1	1	1	G	5	DS-HDV
12	6/9/23	15:00	1	1	1	G	4	DS-HDV
13	6/9/23	16:10	1	1	1	G	4	DS-HDV
14	6/13/23	13:15	1	1	1	Y	2	DS-HDV
15	6/13/23	14:36	1	1	1	Y	2	DS-HDV
16	6/13/23	15:36	1	1	1	Y	2	DS-HDV
17	6/14/23	11:53	1	1	1	N	1	DS-HDV
18	7/11/23	10:54	1	1	1	Y	2	DS-TTT-SAA
19	7/11/23	11:51	1	1	1	Y	2	DS-TTT-SAA
20	7/11/23	14:59	1	1	1	Y	2	DS-TTT-SAA
21	7/11/23	15:10	1	1	1	Y	2	DS-TTT-SAA
22	7/14/23	13:47	1	1	1	N	4	DS-HDV
23	7/14/23	14:45	1	1	1	N	4	DS-HDV
24	7/26/23	10:40	1	1	1	Y	2	DS-TTT-SAA
25	7/26/23	11:32	1	1	1	Y	2	DS-TTT-SAA
26	7/26/23	13:35	1	1	1	Y	2	DS-TTT-SAA
27	7/26/23	14:17	1	1	1	Y	2	DS-TTT-SAA
28	7/26/23	14:53	1	1	1	Y	2	DS-TTT-SAA
29	7/26/23	15:30	1	1	1	Y	2	DS-TTT-SAA

A preliminary discussion of a subset of the dataset is presented here. Initial data from radar and camera data confirm that sensors are operating as expected as shown in Fig. 10 and Fig. 11. Fig. 10 shows the output range vs time plot for detections from radar located on the 1272 rooftop when three SUAS flew a HDV PAO mission.

Takeoff time for the HDV SUAS are staggered and this is reflected in the detection plots. Each SUAS exits the FOV of the rooftop radar yielding the~300 second gaps in the discrete detection plots for each SUAS. Fig. 11 shows the output of the vision detection algorithm for the Wythe Creek location.

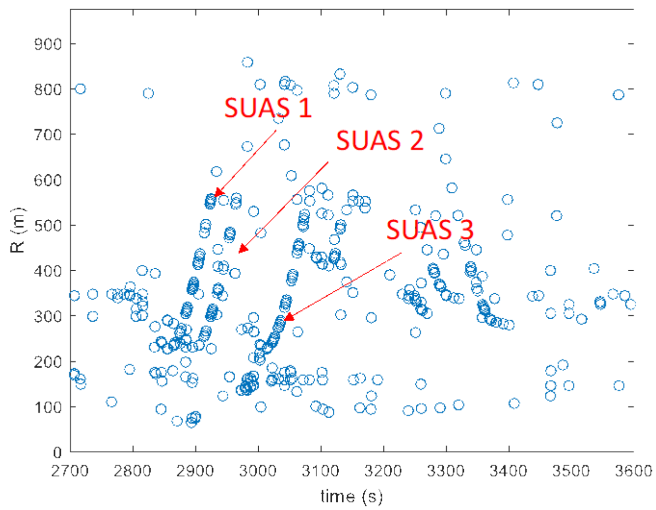

Fig. 10: Sample radar detections of 3 SUAS flying the same waypoint pattern from the 1272 roof top location where the vertical axis Range (R) and time as retrieved using the filtering algorithm in [13].

Fig. 11: Output of detection algorithm from [24] where red are morphological detections and magenta are image differencing detections. The bottom two detections are the HDV SUAS while the upper magenta detection is of an aircraft entering the flight area.

Radar data collected from onboard Alta X from 6/13/2023 is shown in Fig. 12. The airborne radar yielded many more detections compared to the ground-based radars and likely suffered from interference from other radars as there were insufficient channels. The raw detection plot shown in Fig. 12a shows sensor saturation for radar, however, filtering the data by doppler as shown in Fig. 12b helped reduce detections unrelated to SUAS. Finally, using the radar tracking strategy described in [13] revealed tracks correlated with SUAS. The work in [14] presents a distributed radar architecture using data collected from this experiment, including radar interference mitigation strategy.

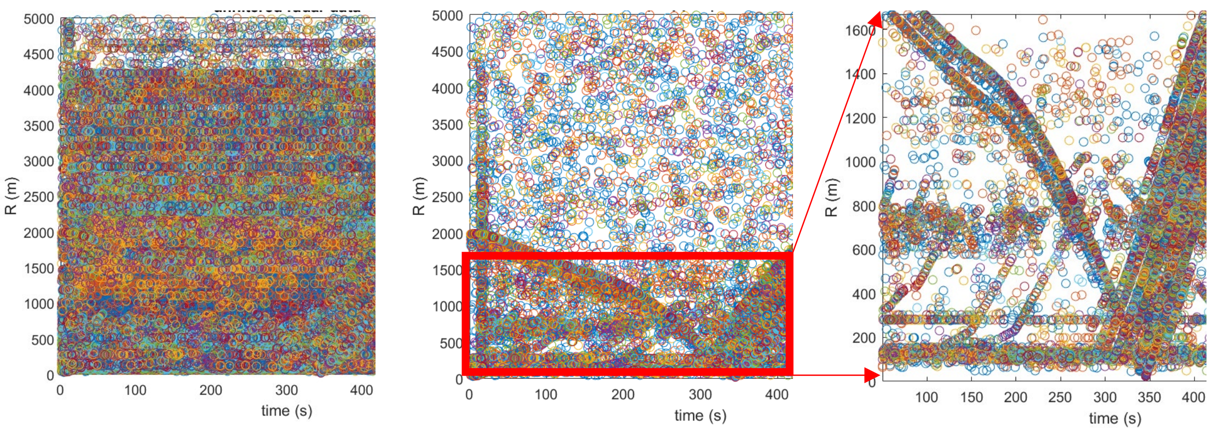

(a) (b) (c)

Fig. 12: Radar interference and filtering from radar on Alta X: a) radar detections b) radar detections filtered to |Doppler| >= 0.9 c) zoomed to CERTAIN range flight space after doppler filtering.

VI. Detect, Track, and Classify Approach

This section describes the performance metrics, vision tracking technique, the radar tracking technique, sensor fusion methodologies, and planned machine learning approaches. Formal sensing requirements for UAM have not been adopted for widespread UAM usage by an aviation authority and remains an area of aviation research. These requirements include defining the range that a SUAS or UAM aircraft needs to be detected from a SUAS or UAM aircraft or from ground-based sensing strategies. The detect, track, and classify strategies are based on existing techniques.

A. Performance Metrics

The distributed sensing framework will be evaluated in terms of detection and tracking coverage of SUAS, precision-recall performance, localization accuracy, and range performance. Additionally, analysis will examine the benefits of sensing from single versus multiple nodes for these performance metrics. Further, performance will be quantified in terms of range. Future work in this domain will include evaluation of this dataset using standard compute vision and machine learning performance metrics along proposed aviation metrics for SUAS from regulatory authorities such as the FAA and RTCA working groups.

B. Vision Acquisition and Processing

The vision detection processing pipeline is described in detail [24] and summarized in Figure 13.

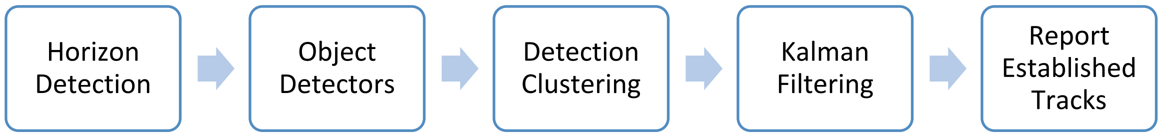

Figure 13: Vision Detection and Tracking Pipeline.

The vision detection pipeline first segments the area below the horizon as the sensors are looking upwards. Next, spatial and temporal object detectors extract objects of interest, then detections are clustered by pixel radius to avoid generating multiple tracks of the same object. Next, the detections either associated with an existing track by an association algorithm or a new track are generated with initial Kalman filter settings, and finally tracks that meet thresholds such as track age (minimum of 1 second) and dropout criteria (minimum detections in at least 50% of the frames) are reported to the multi-sensor tracker.

C. Radar Acquisition and Processing

The Frequency Modulated Continuous Wave (FMCW) radar has a maximum field of view of 120° azimuth and 80° elevation field of view. The radar transmits 2 watts of peak power through a horizontally polarized Metamaterial Electronically Scanning Array antenna with a peak gain of 22 dBi. The radar provides 3 channels of 45 MHz bandwidth each centered at 24.55 GHz with 15 Mhz separation between channels. The radar has independent transmission and reception antenna arrays divided by a small aluminum metal fence to reduce cross talk coupling. The radar firmware version 11 was used during this evaluation. The radars are operated in their "search with track" mode. In this mode the radar logic points the antenna across the entire field of view at predefined increments, ensuring the entire field of view is scanned, and new tracked objects are acquired typically within 1 second. Once an object detection is made at given azimuth and elevation, the radar will collect 4 more acquisitions at beam angles adjacent to the original detection. This sequential lobing technique is used to spatially pinpoint the speed and location of the object being tracked.

D. EKF Tracker Implementation

The Extended Kalman Filter as used for sensor fusion at each node is explained in [25] as shown in Fig. 14 and the distributed node architecture in [11].

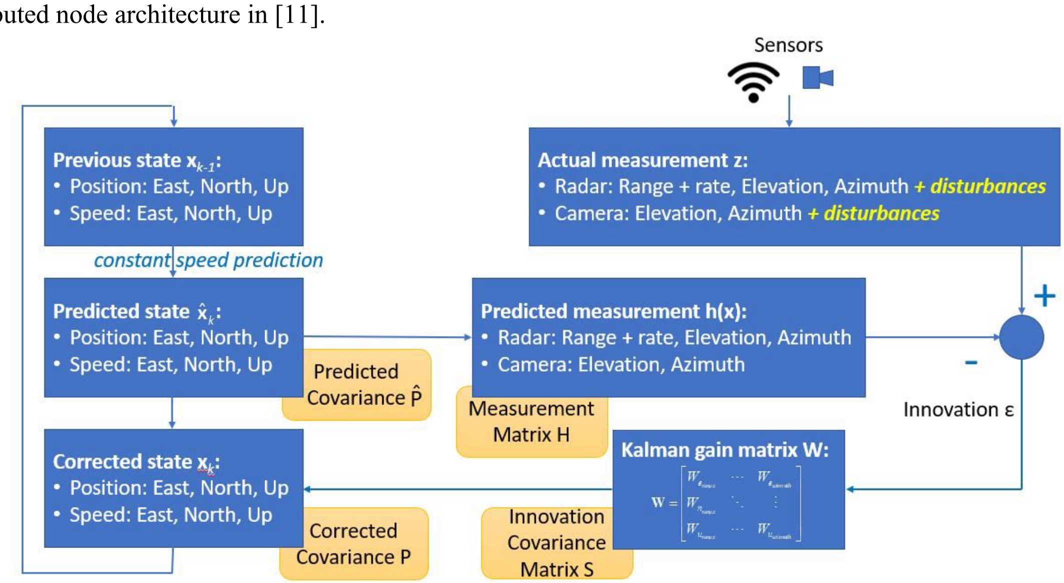

Fig. 14: General Overview of the Kalman Filter setup.

E. Machine Learning Approaches

The output of radar, camera, node level sensor fusion, or distributed fusion pipeline may be classified in an architecture as shown in Fig. 15. Utilizing a detection and tracking scheme to preprocess data for a machine learning algorithm is useful for small object classification as it can reduce the number of computations needed as the entire image does need to be classified and hence fewer convolutions need to be performed. The work in [26] [27] integrates a vision-based detection and track framework with a Convolutional Neural Network (CNN) to perform image classification and achieved higher classification accuracy than a retrained You Only Look Once (YOLO) v4 on the same dataset. A trajectory classification scheme was developed in the work in [28] for radar and will be extended to vision and sensor fusion strategies.

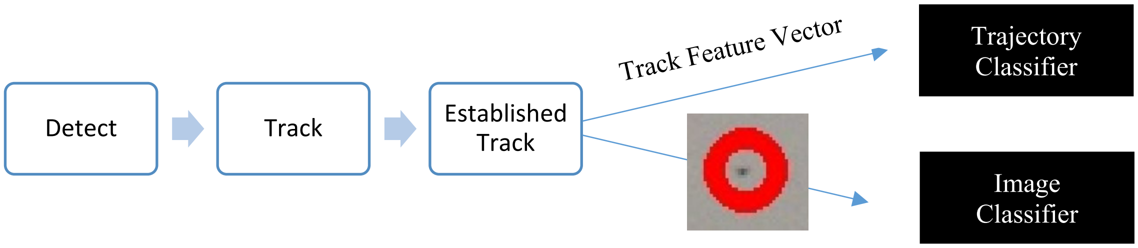

Fig. 15: Two Machine Learning Strategies for Classifying Aircraft and Birds.

VII. Conclusion

This paper presented a distributed sensing system architecture and collected data in partnerships with AAM HDV for distributed system evaluation. Future analysis will include evaluation of the sensing of modalities, detection and tracking strategies, and aerial object classification algorithms. Improved position estimate accuracy of HDV SUAS is expected during simultaneous detections of SUAS from multiple nodes and sensors. Future work includes developing distributed sensing strategies and evaluating the integration of detections at node vs system level. Challenges include filtering radar data to extract detections of aircraft while suppressing abundant undesired detections. Fusing the radar and vision modalities leverages both the high angular resolution capability of the vision sensor and the range information from radar. This dataset will provide an opportunity to evaluate sensing modality performance, different sensing strategy performance, and considerations with placement of distributed sensing nodes in proximity to vertiports in proximity to buildings, trees, and metal structures. Future plans include making the dataset publicly available after preliminary analysis has been completed.

Acknowledgements

The authors would like to thank Lou Glaab and Jacob Shaeffer for facilitating the HDV+TTT joint activity, Matt Coldsnow for his help with safety reviews, Zackary Mitchell for his assistance in data acquisition, Greg Howland for initial CAD work (AMA), SUAS pilots Mark Motter, Jody Miller, and Brayden Chamberlain, Range Safety Officers Mark Frye and Jennifer Fowler, and interns Yajvan Ravan and Aref Malek.

References

[1] W. Johnson and C. Silva, "NASA concept vehicles and the engineering of advanced air mobility aircraft," *The Aeronautical Journal,* vol. 126, pp. 55-91, 2022.

[2] C. Ippolito, K. Hashemi, E. Kawamura, G. Gorospe, W. Holforty, K. Kannan, V. Stepanyan, T. Lombaerts, N. Brown, A. Jaffe and C. Dolph, "Concepts for Distributed Sensing and Collaborative Airspace Autonomy in Advanced Urban Air Mobility," in *AIAA SciTech*, National Harbor, 2023.

[3] D. Locascio, M. Levy, K. Ravikumar, S. Briceno, B. German and D. Mavris, "Evaluation of Concepts of Operations for On-Demand Package Delivery by Small Unmanned Aerial Systems," in *AIAA AVIATION Forum*, Washington DC, 2016.

[4] E. Hunt and S. Rondon, "Detection of potato beetle damage using remote sensing from small unmanned aircraft systems," *Journal of Applied Remote Sensing,* vol. 11, no. 2, pp. 026013-026013, 2017.

[5] S. Dorafshan, R. Thomas, C. Coopmans and M. M., "Deep Learning Neural Networks for sUAS-Assisted Structural Inspections: Feasibility and Application," in *International Conference on Unmanned Aircraft Systems* , Dallas, 2018.

[6] K. Pratt, R. Murphy, S. Stover and C. Griffin, "CONOPS and autonomy recommendations for VTOL small unmanned aerial system based on Hurricane Katrina operations," *Journal of Field Robotics,* vol. 26, no. 8, pp. 636-650, 2009.

[7] S. Ramasamy and R. Sabatini, "A Unified Approach to Cooperative and Non-Cooperative Sense-and-Avoid," in *International Conference on Unmanned Aircraft Systems (ICUAS)*, Denver, 2015.

[8] C. Price, D. Helton, K. Jenkins, M. Kvicala, S. Parker and R. Wolfe, "Urban Air Mobility Operational Concept (OpsCon) Passenger-Carrying Operations," NASA/CR-2020-5001587, 2020.

[9] L. Glaab, M. Johnson, R. McSwain, S. Geuther, Q. Dao and J. Homola, "The high density vertiplex advanced onboard automation overview.," in *IEEE/AIAA 41st Digital Avionics Systems Conference* , Portsmouth, 2022.

[10] V. Aubuchon, K. Hashemi, R. Shively and J. Wishart, "Multi-vehicle (m: N) operations in the NAS-NASA's research plans," in *AIAA Aviation*, Chicago, 2022.

[11] T. Lombaerts, K. Kannan, E. Kawamura, C. Dolph, V. Stepanyan, G. Gorospe and C. Ippolito, "Distributed Ground Sensor Fusion Based Object Tracking for Autonomous Advanced Air Mobility Operations," in *AIAA SciTech*, Washington DC, 2023.

[12] C. Ippolito, E. Kawamura, G. Gorospe, W. Holforty, K. Kannan, V. Stepanyan, T. Lombaerts, N. Brown, A. Jaffe and C. Dolph, "A Structurally-Adaptive Framework for Distributed Airborne Sensing over Real-time Collaborative Information Sharing Networks," in *AIAA SciTech*, Washington DC, 2023.

[13] F. Vitiello, F. Causa, R. Opromolla, G. Fasano, C. Dolph, T. Lombaerts and C. Ippolito, "Assessing Performance of Radar/Visual Fusion Techniques for Ground-to-Air Surveillance in Advanced Air Mobility: an Experimental Approach," in *IEEE/AIAA Digital Avionic Systems Conference*, Barcelona, Spain, 2023.

[14] F. Vitiello, F. Causa, R. Opromolla, G. Fasano, C. Dolph, T. Ferrante, T. Lombaerts and C. Ippolito, "Experimental Testing of Data Fusion in a Distributed Ground-Based Sensing Network for Advanced Air Mobility," in *AIAA SciTech Forum*, Orlando, 2024.

[15] NASA, "ADVANCED AIR MOBILITY (AAM) MISSION," 27 Nov. 2023. [Online]. Available: https://nari.arc.nasa.gov/aam/.

[16] T. Lombaerts, K. Kannan, E. Kawamura, C. Dolph, V. Stepanyan, G. Gorospe and C. Ippolito, "Distributed Ground Sensor Fusion Based Object Tracking for Autonomous Advanced Air Mobility Operations.," in *AIAA SciTech 2023 Forum.*, National Harbod, MD, 2023.

[17] V. Stepanyan, K. Kannan, E. Kawamura, T. Lombaerts and C. Ippolito, "Distributed Target Tracking With Optimal Data Migration," in *AIAA SciTech Forum and Exposition*, National Harbor, MD, 2023.

[18] C. Dolph, T. Lombaerts, E. Kawamura, C. Ippolito, V. Stepanyan, K. Iftekharuddin, G. Szatkowski, R. McSwain, C. Morris, M. Malekpour and C. MInwalla, "Ground to air testing of a fused optical-radar aircraft detection and tracking system," in *AIAA SciTech*, San Diego, 2022.

[19] E. Kawamura, K. K. Dolph, T. Lombaerts and C. Ippolito, "Distributed Sensing and Computer Vision Methods for Advanced Air Mobility Approach and Landing," in *AIAA SciTech 2023 Forum*, National Harbor, MD, 2023.

[20] E. Kawamura, C. Dolph, K. Kannan, T. Lombaerts and C. Ippolito, "VSLAM and Coplanar POSIT for Advanced Air Mobility Approach and Landing," in *AIAA SciTech 2023* , National Harbor, MD, 2023.

[21] B. Petty, J. Unverricht, B. Buck, L. Glaab, Q. Dao and J. Homola, "High Density Vertiplex: Scalable Autonmous Operations Prototype Assessment Simulation," in *AIAA SciTech*, Orlando, 2024 (In Preparation).

[22] N. U. A. I. R. A. (NUAIR), "High-density automated vertiport concept of operations.," NASA, 2021.

[23] B. K. Buck, E. T. Chancey, M. S. Politowicz, J. R. Unverricht and S. C. Geuther, "A remote vehicle operations center's role in collecting human factors data," in *AIAA SciTech*, National Harbor, MD, 2023.

[24] C. Dolph, C. Minwalla, L. Glaab, M. Logan, B. Allen and K. Iftekharuddin, "Detection and Tracking of Aircraft from Small Unmanned Aerial Systems," *Journal of Aerospace Information Systems,* vol. 18, no. 11, pp. 838-851, 2021.

[25] T. Lombaerts, K. Shish, G. Keller, V. Stepanyan, N. Cramer and C. Ippolito, " Adaptive Multi-Sensor Fusion Based Object Tracking for Autonomous Urban Air Mobility Operations," in *AIAA SciTech* , San Diego , 2022.

[26] C. Dolph and E. al, "Adversarial Learning Improves Vision-Based Perception from Drones with Imbalanced Datasets," *Journal of Aerospace Information Systems,* vol. 20, no. 8, pp. 489-507, 2023.

[27] Dolph, C.; Ippolito, C.; Glaab, L.; Logan, M.; Tran, L.; Allen, D.; Alam, M.; Li, J.; Iftekharuddin, K.;, "Adversarial Learning Improves Vision-Based Perception from Drones with Imbalanced Datasets," *JOURNAL OF AEROSPACE INFORMATION SYSTEMS,* vol. 20, no. 8, pp. 489-507, 2023.

[28] H. Holbrook, P. Garrett, N. Behari, C. Dolph, C. Morris and G. Szatkowski, "Aerial Object Trajectory Classification by Training on Flight Controller Data and Testing on RADAR Generated Tracks," in *AIAA SciTech*, San Diego , 2022.

[29] W. Kong, D. Zhang, X. Wang, X. Z. and J. and Zhang, "November. Autonomous landing of an UAV with a ground-based actuated infrared stereo vision system," in *International conference on intelligent robots and systems*, 2013.

[30] D. Comaniciu and P. Meer, "Mean shift: A robust approach toward feature space analysis," *IEEE Transactions on pattern analysis and machine intelligence,* vol. 24, no. 5, pp. 603-619., 2002.

[31] E. Johnson, A. Calise, Y. Watanabe, J. Ha and J. Neidhoefer, "Real-time vision-based relative aircraft navigation," *Journal of Aerospace Computing, Information, and Communication,* vol. 4, no. 4, pp. 707-738, 2007.

[32] C. Li, C. Xu, C. Gui and M. Fox, "Distance regularized level set evolution and its application to image segmentation," *IEEE Transactions on Image Processing,* vol. 19, no. 12, p. 3243–3254, 2010.

[33] R. Malladi, J. Sethian and B. Vemuri, "Shape modeling with front propagation: a level set approach," *IEEE Transactions: Pattern Analysis and Machine Intelligence,* vol. 17, no. 2, pp. 158–175,, 1995.

[34] C. A. Ippolito, K. Hashemi, G. Gorospe, W. Holforty, K. Kannan, V. Stepanyan, T. Lombaerts, N. Brown, A. Jaffe and C. Dolph, "Concepts for Distributed Sensing and Collaborative Airspace Autonomy in Advanced Urban Air Mobility," in *AIAA SciTech Forum and Exposition*, Washington DC, 2023.